ELSEVIER

Optical Materials 19 (2002) 109–116

OPTICAL Materials

www.elsevier.com/locate/optmat

Growth of Ce-doped Colquiriite- and Scheelite-type single crystals for UV laser applications

K. Shimamura [a,*], H. Sato [a], A. Bensalah [a], H. Machida [b], N. Sarukura [c], T. Fukuda [a]

[a] *Institute for Materials Research, Tohoku University, Katahira 2-1-1, Aoba-ku, Sendai 980-8577, Japan*
[b] *Tokin Corporation, Saitama 360-0843, Japan*
[c] *Institute for Molecular Science, Okazaki 444-8585, Japan*

Abstract

Ce-doped Colquiriite- and Scheelite-type fluoride single crystals were grown by the Czochralski technique. The formation of inclusions and cracks accompanying the crystal growth was investigated. The effective distribution coefficients of Ce^{3+} in $LiCaAlF_6$, $LiSrAlF_6$, $LiYF_4$ and $LiLuF_4$ were determined to be 0.031, 0.028, 0.116 and 0.054, respectively. Ultraviolet pulse generations with an output energy of 60 and 27 mJ were obtained from Ce:$LiCaAlF_6$ and Ce:$LiLuF_4$ lasers.

1. Introduction

Coherent optical sources in the ultraviolet (UV) wavelength region are useful for many practical applications, such as medical procedures, semiconductor processing, micromachining, optical communications and remote sensing [1]. Although various kinds of excimar lasers and tunable color center lasers have been investigated as UV sources, their applications are still restricted because they can be used only at low temperature and because of crystal deterioration.

Recently, Ce^{3+} ion-doped fluorides including Colquiriite-type crystals such as $LiCaAlF_6$ (LiCAF) [2,3], and Scheelite-type such as $LiLuF_4$ (LLF) [4,5] have been identified to be efficient and convenient UV solid-state laser media. However, due to the limited size of the available crystals, it was difficult to obtain high energy output directly from a Ce:LiCAF and Ce:LLF laser. The growth of these crystals, especially, is known to be difficult. For the growth of these crystals, a fluorination process using gases such as HF [6] is usually performed in order to purify both raw materials and growing crystals.

We previously reported the growth of Ce:LiCAF crystals without either the use of HF gases or the hydrofluorination of raw materials [7]. Instead, a growth chamber was evacuated to $\approx 10^{-2}$ Torr prior to growth, and high purity Ar (99.9999%) gas was used as a growth atmosphere. Under these conditions, a deposit of a white foreign substance was found on the surface of the

* Corresponding author. Tel.: +81-22-215-3048; fax: +81-22-215-2413.
E-mail address: shimak@imr.edu (K. Shimamura).

0925-3467/02/$ - see front matter
PII: S0925-3467(01)00207-5

grown crystals. The formation mechanism of the white substance was then investigated. In order to avoid its formation and grow high-quality crystals with higher reproducibility, several modifications such as high vacuum atmosphere prior to growth, the use of CF_4 gas instead of Ar, and a growth with a low temperature gradient, were required [8,9].

In the present work, we describe the growth of Colquiriite-type and Scheelite-type single crystals by the Czochralski (CZ) technique under modified growth conditions based on the investigations of Shimamura et al. [7]. Problems accompanying the crystal growth, such as inclusions and cracks, were investigated. High laser performances were achieved using crystals grown in this way.

2. Experimental

Crystal growth was performed in a CZ system with a resistive heater made of high-purity graphite. The starting material was prepared from commercially available AlF_3, CaF_2, SrF_2, LiF, YF_3 and LuF_3 powders of high purity (>99.99%). As dopants, CeF_3 and NaF powders of high purity (>99.99%), were used. Na^+ was co-doped with Ce^{3+} in order to maintain the charge neutrality for Colquiriite-type crystals. The concentration of Ce^{3+} and Na^+ in the starting material was 1 mol%. The starting material was placed in a Pt crucible.

Vacuum treatment was performed prior to growth. The system was heated from room temperature to 700 °C for a period of 12 h under vacuum ($\approx 10^{-5}$ Torr). Both rotary and diffusion pumps were used to achieve $\approx 10^{-5}$ Torr and effectively eliminate water and oxygen from the growth chamber and the starting material. Subsequently, high purity CF_4 gas (99.9999%) was slowly introduced into the furnace. Thereafter, the starting material was melted at approximately 820 °C.

The determination of lattice parameters and the phase identification were performed by the X-ray powder diffraction method (XRD). The dependence of lattice parameters on the temperature was measured by the high temperature XRD method using a RIGAKU RINT 2000 apparatus under vacuum atmosphere. Specimens for XRD analysis were prepared by milling grown single crystals in a mortar. Chemical composition was determined by the induced coupled plasma method. Absorption spectra in the infrared (IR) wavelength region were measured by FT-IR with high resolution. Transmission in the VUV wavelength region at room temperature was analyzed by VUV 5530 spectrophotometry under vacuum.

3. Results and discussion

Fig. 1 shows as-grown Colquiriite-type single crystals, Ce:LiCAF and Ce:$LiSrAlF_6$ (LiSAF) 18 mm in diameter and 60 mm in length. Fig. 2 shows as-grown Scheelite-type single crystals, Ce:$LiYF_4$ (YLF) and Ce:LLF 18 mm in diameter and 60 mm in length. These crystals were grown at pulling and rotation rates of 1 mm/h and 10 rpm, respectively. Cracks, bubbles and inclusions were not observed. Under the modified growth conditions, foreign substances on the surface of the grown crystal, as observed in [7,9], were not formed. However,

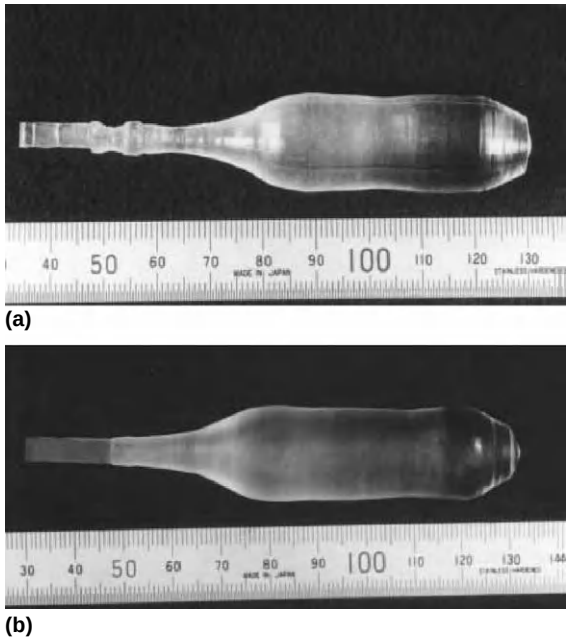

Fig. 1. As-grown Ce-doped: (a) $LiCaAlF_6$ and (b) $LiSrAlF_6$ single crystals of 18 mm in diameter pulled along the *a*-axis.

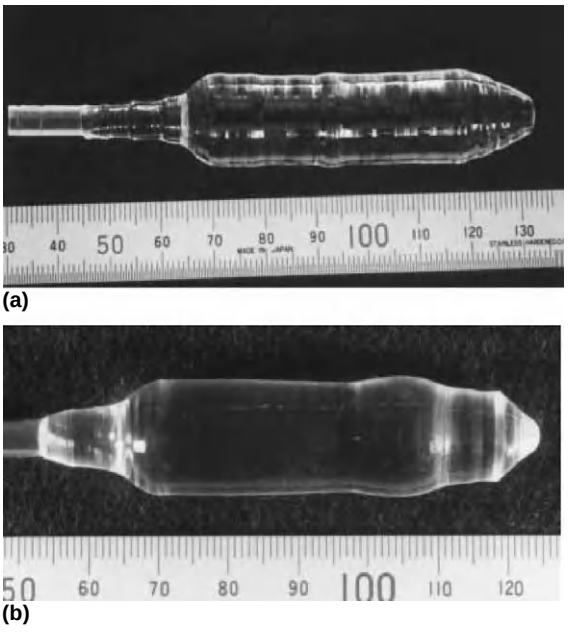

Fig. 2. As-grown Ce-doped: (a) $LiYF_4$ and (b) $LiLuF_4$ single crystals of 18 mm in diameter pulled along the *a*-axis.

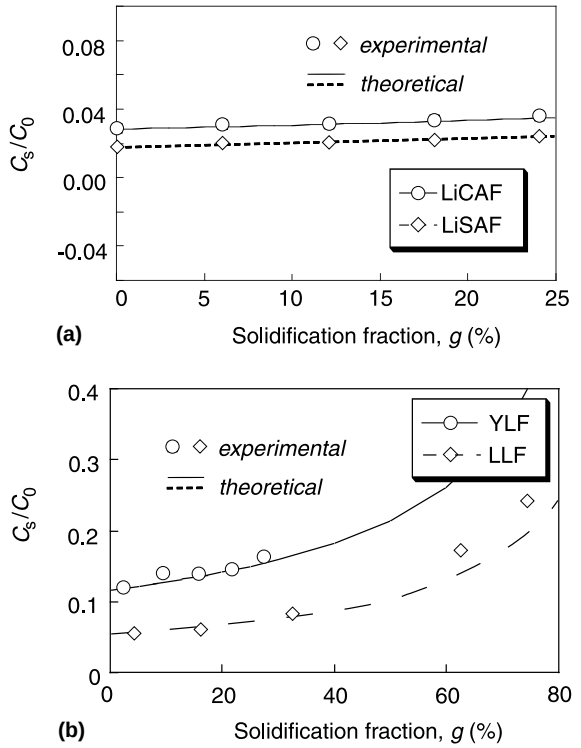

Fig. 3. Concentration dependence of Ce^{3+} on solidification fraction, measured for Ce-doped: (a) $LiCaAlF_6$ and $LiSrAlF_6$, and (b) $LiYF_4$ and $LiLuF_4$ single crystals. C_0 and C_s are the initial concentration and the concentration at each solidification fraction, respectively.

Ce:LiSAF showed a tendency to crack perpendicular to the growth axis after several days. On the contrary, Ce:LiCAF did not show cracks at any time.

Fig. 3 shows the distribution of Ce^{3+} concentration along the growth axis. The effective distribution coefficient (k_{eff}) of Ce^{3+} in LiCAF, LiSAF, YLF and LLF were determined to be 0.031, 0.028, 0.116 and 0.054, respectively, by the following equation [10]:

$$\frac{C_s}{C_0} = k_{eff}(1-g)^{k_{eff}^{-1}}. \quad (1)$$

Solid and dotted lines in Fig. 3 were obtained using Eq. (1). The k_{eff} of Ce^{3+} in LiCAF was larger than in LiSAF. This is because the ionic radius of Ce^{3+} under 6-fold coordination (1.01 Å) is closer to that of Ca^{2+} (1.00 Å) than to that of Sr^{2+} (1.18 Å) [11], the ions thought to be replaced by Ce^{3+} [7]. The k_{eff} of Ce^{3+} in YLF was larger than in LLF. This is because the ionic radius of Ce^{3+} under 8-fold coordination (1.143 Å) is closer to that of Y^{3+} (1.019 Å) than to that of Lu^{3+} (0.977 Å) [11], the ions thought to be replaced by Ce^{3+} [9]. The k_{eff} of Scheelite-type crystals was almost one order larger than that of Colquiriite-type crystals. This is because Scheelite-type crystals do not need charge compensation since Y and Lu has the same valence as Ce.

Fig. 4 shows an as-grown 1 in. in diameter Ce:LiCAF and Ce:LiSAF single crystals, grown at pulling and rotation rates of 1 mm/h and 10 rpm, respectively. Although the Ce:LiCAF single crystal was free from cracks and inclusions, the Ce:LiSAF crystal was not when they were grown under the same conditions. When Ce:LiCAF single crystals of this diameter were grown, the following two problems, not observed for 18 mm in diameter crystals, appeared: formation of inclusions, and cracks accompanied by the formation of an impurity phase at the bottom of the crystal.

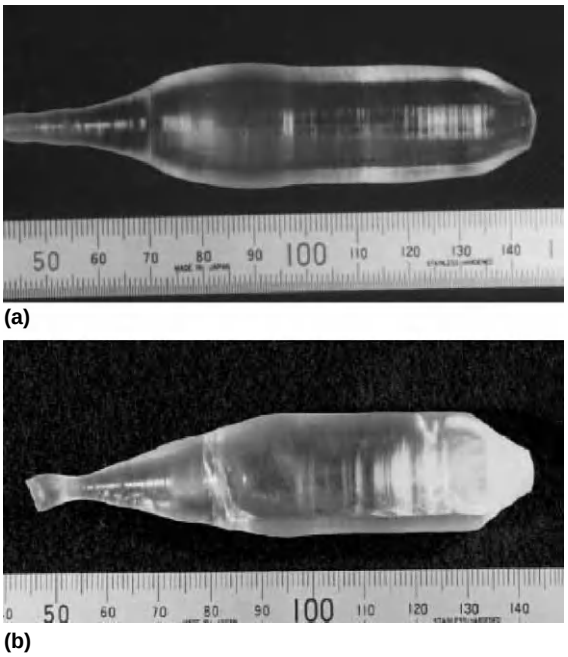

Fig. 4. As-grown Ce-doped $LiCaAlF_6$ and $LiSrAlF_6$ single crystals 1 in. in diameter.

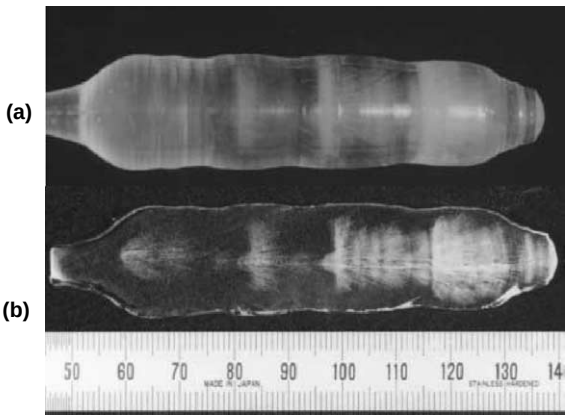

Fig. 5. Ce-doped $LiCaAlF_6$ crystal with inclusions: (a) as-grown crystal and (b) wafer cut parallel to the growth axis.

Fig. 5 shows a polished wafer cut parallel to the growth axis. Many inclusions are distributed throughout the crystal. It should be noticed that the formation of these inclusions was related to a change of the crystal diameter, for example at the shoulder part of the crystal. Once they appeared at the shoulder part, they did not disappear during crystal growth. In order to avoid these inclusions, the diameter at the shoulder part had to be controlled precisely and extended smoothly, without rapid change of the diameter. Fig. 6 shows the absorption spectra for the wafer shown in Fig. 5(b), in regions with and without inclusions. Although the absorption spectrum for the inclusion free region did not show any absorption peaks, that of the region with inclusions had one small absorption peak around 3600 cm^{-1}. Since this peak indicates the existence of OH^- [1], it is thought that H_2O based impurities were present in the inclusions.

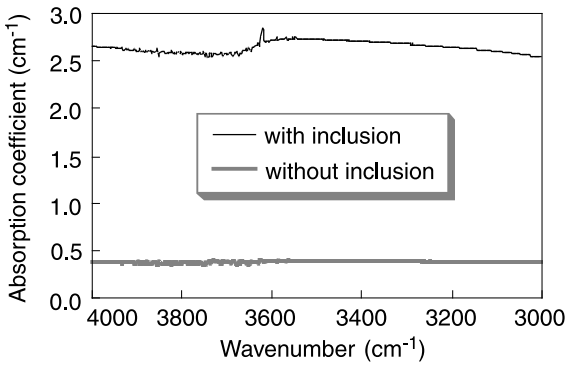

Fig. 6. Infrared absorption spectra of the crystal shown in Fig. 5.

Fig. 7 shows an as-grown crystal with one large crack along the growth axis and a white substance at the bottom of the crystal. This large, flat crack appeared during cooling after growth, in cases when white material was present. This white substance usually formed when the solidification

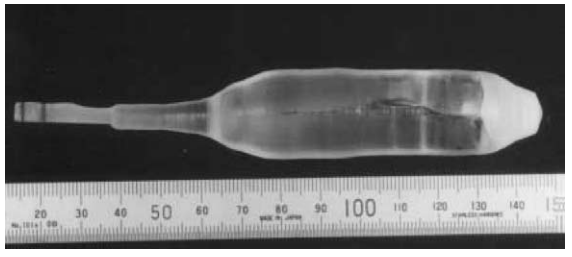

Fig. 7. As-grown Ce-doped $LiCaAlF_6$ single crystal with white substance at the bottom of the crystal and a large crack parallel to the growth axis.

fraction exceeded 70%. The XRD analysis showed that the white substance was composed of LiCAF and CaF_2 phases. This is because the melt composition shifted in the CaF_2-enriched direction during growth, since the vaporization pressure of LiF and AlF_3 is very high [12]. CeF_3 and NaF might have accumulated in the residual melt due to the small k_{eff}. In order to avoid formation of this white substance, crystal growth was terminated at the solidification fraction 60%, as with the crystal shown in Fig. 4.

Fig. 8 shows the dependence of the lattice parameters a and c on the temperature. In the case of LiCAF crystals, at a temperature below 600 °C, only the LiCAF phase existed, while above 700 °C, the compound was completely decomposed to Li_3AlF_6, CaF_2 and Al_2O_3. It was considered that Al_2O_3 was synthesized by the presence of a small amount of water or oxygen in the system. Therefore, thermal expansion was evaluated only up to 600 °C. LiSAF crystals also showed the same phenomena as LiCAF. The calculated linear thermal expansion coefficients α_{11} and α_{33} are listed in Table 1. There is a notable difference between the linear thermal expansion coefficient along the a-axis and along the c-axis of LiCAF crystals. The latter is $\alpha_{33} = 2.5 \times 10^{-6}$ °C^{-1}, which is only about 10% of the former, $\alpha_{11} = 22.9 \times 10^{-6}$ °C^{-1}. Further, the thermal expansion of LiSAF was highly anisotropic, due to the thermal expansion along the c-axis being negative, i.e. the lattice parameter c decreases with increasing temperature. These results suggest that large diameter LiSAF crystals are difficult to grow from the melt because of thermal stress inside the grown crystals. No distinct difference in the linear thermal expansion coefficients was observed between undoped crystals and Ce-doped ones. Based on these considerations, 2-in. Ce:LiCAF single crystals were investigated.

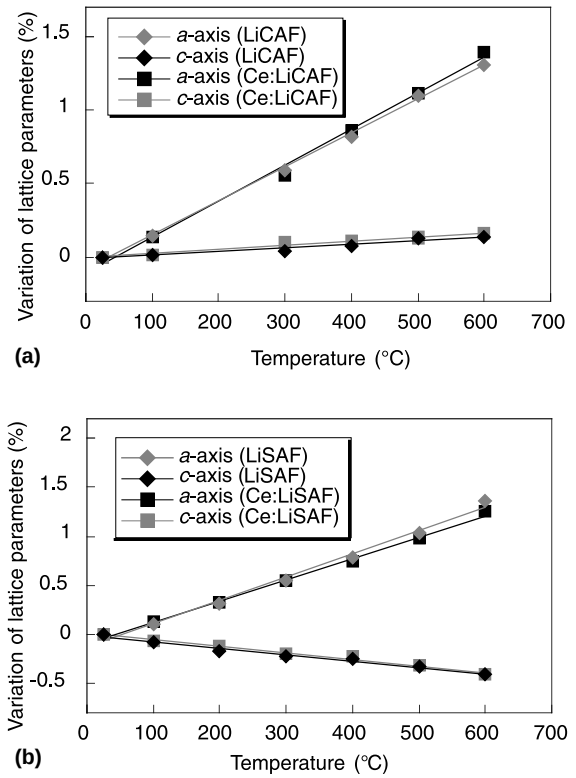

Fig. 8. Temperature dependence of the lattice parameters a and c for: (a) $LiCaAlF_6$ and (b) $LiSrAlF_6$ single crystals.

Table 1
Linear thermal expansion of undoped and Ce-doped $LiCaAlF_6$ and $LiSrAlF_6$ single crystals

	Linear thermal expansion coefficients ($\times 10^{-6}$ °C^{-1})	
	α_{11} (along the a-axis)	α_{33} (along the c-axis)
$LiCaAlF_6$	22.9	2.5
$LiSrAlF_6$	23.5	−6.6
Ce:$LiCaAlF_6$	24.3	2.7
Ce:$LiSrAlF_6$	21.6	−6.7

When 2 in. in diameter Ce:LiCAF single crystals were grown, the following two problems appeared: the formation of inclusions, and cracks accompanied by the formation of an impurity phase at the bottom of the crystal. Since these problems were similar to the growth of 1 in. in diameter crystals, they were solved in a same way.

Fig. 9 shows an as-grown 2 in. in diameter Ce:LiCAF single crystal, free from cracks and inclusions, grown at pulling and rotation rates of 0.8 mm/h and 10 rpm, respectively. By improving the growth conditions, such as the precise control of crystal diameter to avoid the formation of inclusions and the termination of crystal growth at the

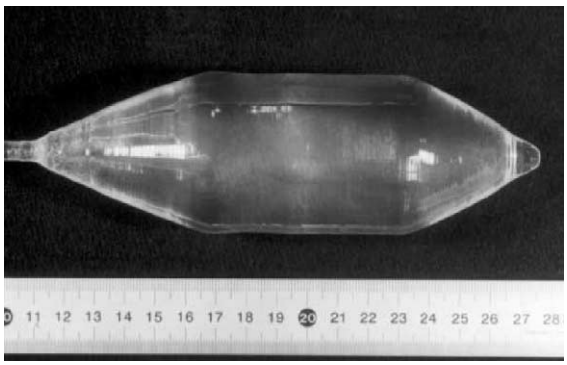

Fig. 9. As-grown Ce-doped $LiCaAlF_6$ single crystal 2 in. in diameter.

solidification fraction of 60% to avoid the formation of the white substance at the bottom of crystal, crystals shown in Fig. 9 could be obtained reproducibly.

Fig. 10 shows the absorption spectra of Ce-doped Colquiriite-type and Scheelite-type crystals. Ce-doped Colquiriite-type crystals can be pumped by the fourth harmonic (4ω) of the Nd-doped $Y_3Al_5O_{12}$ (YAG) laser, since they have an absorption peak at around 266 nm. Although Ce-doped Scheelite-type crystals cannot be pumped in this way, they can be pumped by the KrF excimer laser (248 nm) and/or the fifth harmonic of the Nd:YAG laser.

We have already demonstrated an output energy of 30 mJ from a UV solid-state Ce:LiCAF laser that operated at 290 nm at a repetition rate of 10 Hz [7,13]. In order to obtain higher output energy, we increased the pumping energy. The laser resonator was formed by a flat high reflector and a flat output coupler with 30% reflectivity, separated by 4 cm as shown in Fig. 11. The large Ce:LiCAF crystal (aperture 15 mm × 10 mm) was located midway between the two cavity end mirrors. The 4ω of two simultaneously Q-switched Nd:YAG lasers were used as pumping sources. The three pump beams were focused with a 40-cm focal length lens to produce a spot size of 6 mm at the surface of the Ce:LiCAF crystal. We obtained 60 mJ at 10 Hz, to our knowledge the highest performance so far reported for Ce:LiCAF.

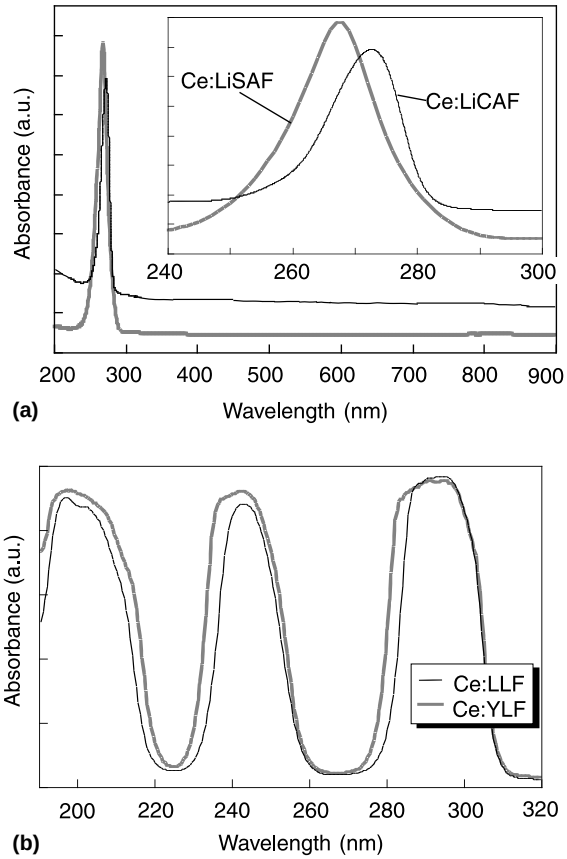

Fig. 10. Absorption spectra of Ce-doped: (a) $LiCaAlF_6$ and $LiSrAlF_6$, and (b) $LiYF_4$ and $LiLuF_4$ single crystals.

Fig. 12 shows the Ce:LLF laser resonator which was established by a flat high reflector and a flat output coupler. The 10-mm Ce:LLF active medium was cut from the as-grown boule in the middle along its axis. The pumping pulses of a randomly polarized KrF excimer laser, which operated at 248 nm with a 1 Hz frequency, were softly focused on the Ce:LLF side window by a spherical lens with 50 cm focal lens in normal incidence. The best results were obtained with a 6 cm cavity and output coupler with 45% transmission. The maximum output power at 309 nm was 27 mJ with pumping pulse energy of 230 mJ; the corresponding pumping fluency was approximately 0.6 J/cm^2. The slope efficiency was approximately 17%. This is the highest output power obtained directly from a Ce:LLF laser re-

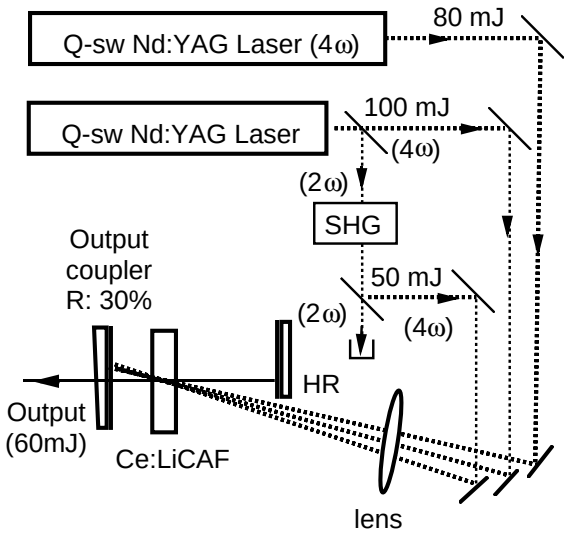

Fig. 11. Experimental setup of a high-energy Ce:$LiCaAlF_6$ laser.

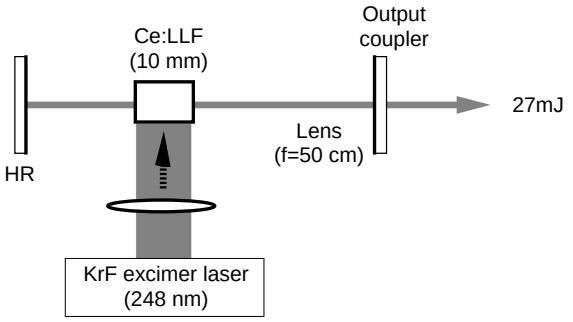

Fig. 12. Experimental setup of a high-energy Ce:$LiLuF_4$ laser.

ported until now. Ce:LLF tunability was also investigated. Laser tunability was obtained in the ranges 307.8–311.7 nm and 323.5–326.5 nm when the pumping energy reached 100 mJ. This tuning regime was similar to that obtained in [14] where a Ce:LLF was pumped by the fifth harmonic of a Nd:YAG laser.

4. Summary

Ce:LiCAF, Ce:LiSAF, Ce:YLF and Ce:LLF single crystals of 18 mm in diameter were grown by the CZ technique under CF_4 atmosphere. Ce:LiSAF showed a tendency to crack more easily than Ce:LiCAF. Although lattice parameters of both the *a*-axis and *c*-axis increased linearly depending on a temperature in the case of LiCAF, that of the *c*-axis decreased in the case of LiSAF. Linear thermal expansion coefficients of both LiCAF and LiSAF were evaluated using the temperature dependence of the lattice parameter. The effective distribution coefficients of Ce^{3+} in LiCAF, LiSAF, YLF and LLF were determined to be 0.031, 0.028, 0.116 and 0.054, respectively. Under the same growth conditions, Ce:LiCAF single crystals of 50 mm in diameter (2 in.) were also grown up to a solidification fraction of 60%. Although numerous inclusions appeared during growth, precise diameter control prevented their formation. Laser output energy of 60 and 27 mJ were obtained using the grown Ce:LiCAF and Ce:LLF single crystals, respectively. These demonstrate that Ce:LiCAF and Ce:LLF are promising materials for high-energy UV pulse generation.

References

[1] N. Sarukura, M.A. Dubinskii, Z. Liu, V.V. Semashko, A.K. Naumov, S.L. Korableva, R.Y. Abdulsabirov, K. Edamatsu, Y. Suzuki, T. Itoh, Y. Segawa, IEEE J. Sel. Top. Quantum Electron. 1 (1995) 792.
[2] M.A. Dubinskii, V.V. Semashko, A.K. Naumov, R.Y. Abdulsabirov, S.L. Korableva, in: A.A. Pinto, T.Y. Fan (Eds.), OSA Proceedings of the Advanced Solid-State Lasers, vol. 15, Optical Society of America, Washington, DC, 1993, p. 195.
[3] M.A. Dubinskii, V.V. Semashko, A.K. Naumov, R.Y. Abdulsabirov, S.L. Korableva, J. Mod. Opt. 40 (1993) 1.
[4] M.A. Dubinskii, R.Y. Abdulsabirov, S.L. Korableva, A.K. Naumov, V.V. Semashko, in: International Quantum Electronics Conference, Optical Society of America, Washington, DC, 1992, Paper FrL2.
[5] M.A. Dubinskii, R.Y. Abdulsabirov, S.L. Korableva, A.K. Naumov, V.V. Semashko, Laser Phys. 4 (1994) 480.
[6] R.F. Belt, R. Uhrin, J. Cryst. Growth 109 (1991) 340.
[7] K. Shimamura, N. Mujilatu, K. Nakano, S.L. Baldochi, Z. Liu, H. Ohtake, N. Sarukura, T. Fukuda, J. Cryst. Growth 197 (1999) 896.
[8] S.L. Baldochi, K. Shimamura, K. Nakano, N. Mujilatu, T. Fukuda, J. Cryst. Growth 200 (1999) 521.
[9] S.L. Baldochi, K. Shimamura, K. Nakano, N. Mujilatu, T. Fukuda, J. Cryst. Growth 205 (1999) 537.

[10] J.S. Shah, in: B.R. Pamplin (Ed.), Crystal Growth and Characterization, vol. 6, Pergamon, Oxford, 1975, p. 114 (Chapter 4).
[11] R.D. Shannon, Acta Cryst. A32 (1976) 751.
[12] D. Klimm, P. Reiche, in: Proceedings of International Symposium on Laser and Nonlinear Optical Materials, November 3–5, 1997, p. 284.
[13] Z. Liu, S. Izumida, H. Ohtake, N. Sarukura, K. Shimamura, N. Mujilatu, S.L. Baldochi, T. Fukuda, Jpn. J. Appl. Phys. 37 (1998) L1318.
[14] N. Sarukura, Z. Liu, S. Izumida, M.A. Dubinskii, R.Y. Abdulsabirov, S.L. Korableva, Appl. Opt. 37 (1998) 6446.